Control strategies for the selective precipitation of $CaCO_3$ from multi-ion solutions

Chinmay Hegde[1]; Andreas Voigt[1]; Kai Sundmacher[1,2]

[1] Institute of Process Engineering, Otto von Guericke University, Magdeburg
[2] Max Planck Institute for Dynamics of Complex Technical Systems, Magdeburg

Corresponding Author: Chinmay Hegde (chinmay.hegde@ovgu.de)

1. Abstract

With rising atmospheric CO_2 levels, carbon dioxide capture through calcium carbonate ($CaCO_3$) precipitation offers a viable pathway for permanent CO_2 storage and the production of useful industrial materials. This study presents the experimental implementation of selective $CaCO_3$ precipitation from multi-ion solutions in a semi-batch operation. The objective is to develop and further implement an autonomous control strategy for the selective precipitation using mine wastes. Two distinct pH control strategies were developed and evaluated: a pH swing approach and a pH constant approach. Both methods prove effective for the precipitation of $CaCO_3$ selectively from different multi-ion solutions rich in Mg^{2+}. The two strategies, however, differ in their precipitation mechanisms. The pH swing method induced rapid nucleation under high supersaturation, producing fine particles predominantly with Calcite morphology. In contrast, the constant-pH method allowed for a slower, controlled growth following initial nucleation, resulting in larger particles with a well-defined bimodal particle size distribution (PSD). Initial development of the strategies done using model solutions that mimics real mine tailing extraction solutions and later validated with actual tailing extraction solutions. Depending on the target particle size, morphology, and process control requirements, either approach can be tailored for specific applications.

Keywords: Selective precipitation, control strategy, $CaCO_3$, pH swing and pH constant strategy

2. Introduction

Calcium carbonate is a versatile and indispensable material in numerous industries [1]. It plays a critical role in construction as a key component for cement and lime, in agriculture as a soil conditioner, as a filler in the paper industry, as a calcium source, and as an inert filler in pharmaceuticals [2], [3], [4]. Solid $CaCO_3$ can be achieved through various methods, including mining natural sources and through synthetic processes such as the carbonation of lime [5], [6]. However, the precipitation of $CaCO_3$ has emerged as a prominent method for producing high-purity $CaCO_3$ tailored for specific industrial applications [7], [8]. The precipitation of calcium carbonate involves controlled chemical reactions to transform dissolved calcium ions into solid carbonate, capturing atmospheric CO_2 through carbon mineralization [9]. This method is particularly attractive because it utilizes calcium-rich industrial wastes and mine tailings, offering a sustainable approach to resource recovery, separation, and utilization [10]. Calcium is available in natural minerals as silicates, mostly Augite ($CaMgSi_2O_6$ + Fe, Al) and

Wollastonite ($CaSiO_3$). In addition, many industrial wastes like ashes, rich in calcium can be used as feedstocks for mineral carbonation [11].

Controlled selective precipitation of $CaCO_3$ is particularly critical while dealing with mine tailings or waste solutions containing a variety of dissolved ions along with the needed calcium ions. For example, waste solutions from mine tailings and industrial effluents often contain a variety of dissolved ions such as sulphate (SO_4^{2-}), iron (Fe^{3+}), magnesium (Mg^{2+}), manganese (Mn^{2+}), and phosphate (PO_4^{3-}), which can interfere with the selective precipitation of $CaCO_3$ [12], [13], [14] [15]. For the precipitated $CaCO_3$ to be used as raw material for the abovementioned purposes, selectively precipitating pure $CaCO_3$ from such multicomponent systems is a critical challenge. The optimal control of the precipitation process depends on precisely regulating various parameters to ensure process efficiency and product quality. The key factors influencing the process include pH, ion concentration, and mixing conditions [16]. Calcium ion extraction is preferred at low pH conditions by use of acids, while carbonate precipitation is more favoured at higher pH conditions [17]. Maintaining an alkaline pH (typically 8.5 to 10.5) is critical, as it promotes the conversion of dissolved CO_2 into carbonate and bicarbonate ions, facilitating $CaCO_3$ precipitation [18]. However, excessively high pH can lead to the co-precipitation of other compounds, necessitating careful monitoring and adjustment [19].

In this study we implemented a semi-batch mode of operation for the selective precipitation of $CaCO_3$ from a mixture solution of various ions. Semi-batch operation is a preferred mode for controlled precipitation due to its ability to provide gradual and precise addition of reactants. This approach ensures uniform mixing and prevents localized supersaturation, which could result in undesired by-products or inconsistent crystal properties. For instance, [20] investigated semi-batch processes for calcium oxalate precipitation, highlighting the advantages of precise reactant addition and enhanced control over crystal growth. Similarly, studies on barium sulphate [21] and magnesium carbonate precipitation [22] have demonstrated the efficacy of semi-batch operation in achieving uniform particle size distribution and desired crystal morphologies. $CaCO_3$ also exhibits three main morphologies: Calcite, Vaterite, and Aragonite. Several factors, such as the reaction rate, pH, ion concentration, temperature, and impurities, influence the morphology of the crystals. For e.g., presence of impurities such as magnesium in the solution favour Vaterite and Calcite [23], while potassium favours needle like structured Aragonite [24]. Similarly, Calcite is favoured in alkaline pH ranges [25], while acidic conditions may favour Vaterite and Aragonite [23]. In these previous studies, the precipitation of the $CaCO_3$ was implemented by directly mixing two solutions, one a source of Ca, such as $CaCl_2$, while the other solution is rich in CO_3^{2-} ions, such as Na_2CO_3 [26]. Due to the very low solubility of $CaCO_3$, it would precipitate without the need for pH regulation. However, while tailing solutions are used to produce $CaCO_3$, other impurities could be co-precipitated [27]. So, the pH regulation via the semi-batch mode not only helps with the controlled selective precipitation of $CaCO_3$, but the rate of precipitation is also beneficial in influencing the phase of the precipitate crystals.

The controlled precipitation of $CaCO_3$ is a critical step in developing an autonomous process control chain, particularly when using complex and variable feedstocks such as mine tailings. These feedstocks fluctuate in ion content, composition, and pH, which can significantly influence nucleation, crystal growth, and the morphology of the precipitated CaCO3. High concentrations of Ca^{2+} ions and impurities, and increase in the pH result in higher supersaturation facilitating nucleation [26]. Thus, an autonomous control of the precipitation

process offers an optimal control of the precipitation process ensuring consistent product quality and operational efficiency in industrial applications. Variability in tailings and waste streams can lead to inconsistent $CaCO_3$ formation, reducing process efficiency and increasing operational costs. By integrating process modelling with an autonomous control chain, we can dynamically adjust operational parameters to maintain optimal precipitation conditions and produce high-purity $CaCO_3$ in a reliable and cost-effective manner.

The study aimed to develop optimal control strategies for creating an autonomous process chain for the selective precipitation of $CaCO_3$ using a complex solution mixture of different species. Two optimal strategies were developed and compared for the optimal control of the precipitation process, focusing on enhancing efficiency and selectivity. Also, the particle size distribution (PSD), the morphology, and the precipitation phenomenon of $CaCO_3$ crystals were analysed for the two optimal control strategies. Furthermore, the impact of foreign ions and impurities on the precipitation process in a model solution containing known species such as Mg^{2+}, etc, was analysed. Additionally, the research demonstrated that the developed profiles could be applied to extraction solutions from actual mine tailings, showcasing their potential to selectively precipitate $CaCO_3$ with high purity, offering a practical approach for resource recovery in mining operations.

3. Theory

The implementation of the pH-swing method for the selective precipitation of $CaCO_3$ in a complex multi-ion mixture solution is governed by the dependency of the solubility of $CaCO_3$ on the pH. Calcium carbonate precipitation occurs when Ca^{2+} ions react with CO_3^{2-} ions dissociated from dissolved atmospheric CO_2:

$$Ca^{2+} + CO_3^{2-} \rightarrow CaCO_3 \tag{1}$$

For the $CaCO_3$ formed to be precipitated, its concentration in the solution should exceed the solubility factor (K_{sp}), which is defined by the product of the ion activity coefficients at equilibrium [28]:

$$K_{sp} = [Ca^{2+}]_{sat}[CO_3^{2-}]_{sat} \tag{2}$$

The K_{sp} of $CaCO_3$ at 25°C in water (at pH 7) is 4.8×10^{-9} [29]. The equilibrium conditions are altered due to the changes in pH, temperature, or ion concentration. When the concentrations of Ca^{2+} and CO_3^{2-} exceed the saturation limits, the solution is supersaturated. Thus, the supersaturation ratio (σ), which is the driving force for precipitation, is defined as [26]:

$$\sigma = \frac{[Ca^{2+}][CO_3^{2-}]}{K_{sp}} \tag{3}$$

This Equation reveals that when the ion activity product exceeds K_{sp} (the ion activity product at equilibrium), $CaCO_3$ precipitates. The supersaturation ratio (σ) is crucial also because its values dictate the phenomenon through which the precipitation process will progress. The precipitation could occur through the primary nucleation, where a large number of nuclei are born spontaneously. This birth phenomenon occurs when the supersaturation ratios are very high and birth rate, B is empirically defined in terms of σ as [30]:

$$B = k_b(\sigma - 1)^n \tag{4}$$

where k_b is the rate constant, and n is the exponential factor. Primary nucleation via birth is a very complex and spontaneous process and is difficult to control. Several previous studies have tried to estimate experimentally the birth rates and found the values of n to be in the range of 8 - 9, and the value of k_b to be around $5.5*10^{-9}$ [31].

The precipitation phenomenon could also progress through growth when the value of σ is not too high [30]. This is a slower process where the excess $CaCO_3$ from the solution attaches to the surfaces of the existing nuclei, and the overall size of the crystals increases. The growth rate G, is calculated as [30]:

$$G = k_g(\sigma - 1)^g \tag{5}$$

where k_g is the growth constant, and g is the exponential constant depending on the growth mechanism (generally between 1 and 2) [30].

From Equation (3), we also see that the precipitation amount depends not only on the Ca^{2+} ion concentration but also on the availability of CO_3^{2-} ions, which is heavily influenced by the pH. The availability of CO_3^{2-} ions is determined by the equilibrium of dissolved carbon dioxide CO_2 in water, which undergoes a series of reactions:

$$CO_2 + H_2O \overset{K_H}{\leftrightarrow} H_2CO_3 \overset{K_1}{\leftrightarrow} H^+ + HCO_3^- \overset{K_2}{\leftrightarrow} 2H^+ + CO_3^{2-} \tag{6}$$

where K_H is the Henry constant for CO_2 dissolution in water, while K_1 and K_2 are the first and the second dissociation constants for H_2CO_3, respectively. The values for the constants are detailed in Table 1.

Table 1: Reaction equilibrium constants at 25 °C [32], [33]

Reaction constant	Symbol	Value
Henry constant	K_H	0.0034 mol/L
1st dissociation constant	K_1	$10^{-6.35}$
2nd dissociation constant	K_2	$10^{-10.3}$

Thus, the concentration of the total dissolved carbonates (C_T) is:

$$C_T = H_2CO_3 + HCO_3^- + CO_3^{2-} \tag{7}$$

Under steady-state conditions, the different carbonate species are at equilibrium depending on the solution pH [34]. From Equation (6) & (7), the equilibrium concentration of CO_3^{2-} ions can be expressed as:

$$[CO_3^{2-}] = \frac{C_T K_1 K_2}{[H^+]^2 + K_1[H^+] + K_1K_2} \tag{8}$$

where [H+] is the proton concentration and the driving force for the pH regulation. This relationship explains the influence of pH on the supersaturation ratio (σ). As the pH decreases, the equilibrium shifts toward H_2CO_3 and HCO_3^-, reducing the concentration of CO_3^{2-} ions. This suppresses $CaCO_3$ precipitation and can even dissolve existing solid $CaCO_3$. Conversely, at higher pH (lower $[H^+]$), the equilibrium favours the formation of CO_3^{2-} ions, increasing supersaturation and promoting $CaCO_3$ precipitation.

3.1. CO_2 dissolution constant

The CO_3^{2-} needed for the precipitation process is supplied by bubbling the CO_2 into the solution. Thus, the concentration of CO_3^{2-} in the solution not only depends on the pH of the solution but also on the total carbonates on the solution (C_T) which in turn depends on the amount of total dissolved CO_2. The concentration of dissolved CO_2 in solution depends on the partial pressure of CO_2 (g) and dissolution capability of the gas governed by the temperature-dependent Henrys constant (K_H). According to Henry's law, the dissolved CO_2 concentration is:

$$C_{CO_2} = K_H p_{CO_2} \tag{9}$$

At ambient pressure and temperature conditions (25°C and 1 bar pressure), the partial pressure of CO_2 in the gas phase is about 400 ppm [35]. However, the partial pressure of CO_2 can be increased without increasing the system pressure by bubbling CO_2 continuously into the solution. Thus, when the partial pressure of CO_2 increases to 100%, the maximum amount of CO_2 that can remain in dissolved form is 0.034 mol/L, from Equation (9). This is also the limiting case for the concentration of carbonate ion in the solution at 1 bar pressure and very high pH [32].

4. Experimental and methods

4.1. Materials

Two distinct sample solution types were used in this study to develop a control chain for the selective precipitation of $CaCO_3$ by capturing atmospheric CO_2 into mine tailings extracts. These include a real mine tailing extract prepared to study the extraction and filtration by the partner university of KIT [36] and several model solutions prepared from different concentrations of $CaCl_2$ and $MgCl_2$ to mimic the mine tailing extracts. These samples were selected to cover a range of conditions and compositions relevant to both controlled and practical applications.

The mine tailing extraction solution was prepared at the Karlsruhe Institute of Technology (KIT). The solution was prepared to study the extraction efficiency of Ca^{2+} ions using different acids for dissolving the tailing concentrations. HCl solution with the stoichiometric coefficient of 1.0 was found to be most effective in extracting Ca^{2+} ions. More about the leaching process can be found in the recent publication [36]. After extraction, the clear solution filtered from the slurry was sent to us for the implementation of the selective precipitation. The concentration of the ions present in the extraction solution were measured using Ion chromatography and found to be 0.06307 mol/L and 0.0061 mol/L for Ca^{2+} and Mg^{2+}, respectively.

The model solution was explicitly prepared to facilitate the study of precipitation under controlled conditions. This approach was chosen due to the easy accessibility of the required chemicals and the ability to produce large quantities of solutions, which are essential for comprehensive experimentation. The calcium-rich model solution was prepared by mixing calcium chloride dihydrate ($CaCl_2.2H_20$) from Carl Roth GmbH + Co. KG (Karlsruhe, Germany) with MiliQ water from Merck Millipore (Massachusetts, US). The pH of the solution is neutral, and to study the influence of impurities on the selective precipitation of $CaCO_3$, different concentrations of Mg^{2+} was used. Magnesium impurities were added in various concentrations to the solution as magnesium chloride ($MgCl_2$) from Carl Roth GmbH + Co. KG (Karlsruhe, Germany). The concentration of Ca^{2+} ions and impurities (Mg^{2+}) in the model solution were kept in the range of concentrations of these ions in that of the actual mine tailings

for the study. All the substances were well mixed with the magnetic stirrer to form a clear solution without any dissolved particles. In contrast to the model solution, the extraction solutions prepared by KIT required additional processing, including filtration, after the extraction step to remove particulate matter and ensure the clarity of the solutions. This additional step emphasized the practical challenges associated with handling real mine tailing extracts, further highlighting the utility of the model solution for preliminary and large-scale testing.

For the shifting of the pH of the solution (model and mine tailing extract) to alkaline ranges, 1M NaOH solution (at pH 13.29) was used. The NaOH solution was prepared by mixing solid NaOH crystal from Merck KGaA (Darmstadt, Germany) with the MilliQ water. Similarly, for the pH shift of the solution to acidic range, 25% HCl solution from Carl Roth GmbH + Co. KG (Karlsruhe, Germany) was used. The CO_2 gas from Linde GmbH (Pullach, Germany) was used as the source for the CO_2 for the carbonate precipitation process.

4.2. Experimental setup and procedure

The carbonate precipitation experiments were carried out in a stirred reactor in an open system setup. The reactor was operated in a semi-batch mode to provide precise control over the reaction conditions necessary for the selective precipitation of $CaCO_3$. The reactor, equipped with a stirrer to ensure homogeneous mixing, was maintained at a constant room temperature. The reactor was provided with a high-pressure resistant glass window for viewing the reaction condition. This setup, Figure 1, allowed for the gradual and controlled addition of reactants, which is critical for achieving uniform supersaturation and avoiding localized conditions that could lead to the formation of undesired by-products.

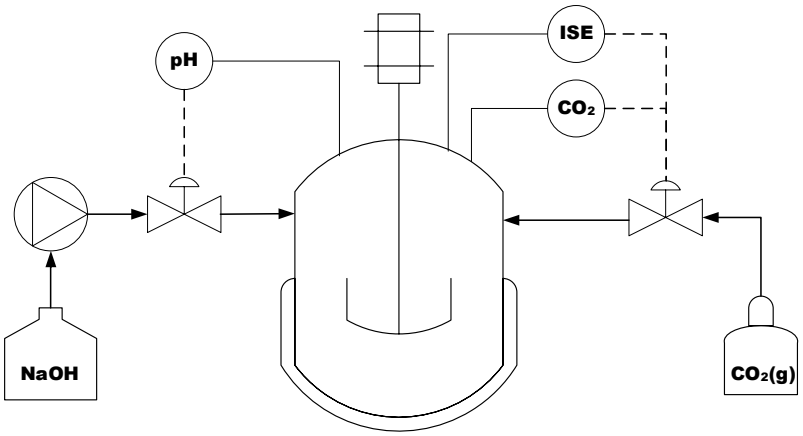

Figure 1: Experimental setup for selective $CaCO_3$ precipitation

The control profiles for the carbonation process is based on the pH of the solution. The setup provided for the continuous measurement of the solution pH using a calibrated pH sensor, pH electrode InLab® Expert Go-ISM, by Mettler Toledo (Ohio, US). For the pH-swing implementation, NaOH solution was supplied through a diaphgram liquid dosing pump, SIMDOS® 10 FEM 1.10 S by KNF Holding AG (Schenkon, Switzerland). The measurement of the change in the concentration of Calcium ion during the experiment is a critical factor for the control of the selective precipitation and the important stopping criteria for the process. Hence the Ca^{2+} ion concentration must be continuously monitored. This was achieved by using calcium ion selective electrode (ISE), DX240-Ca ISE half-cell electrode by Mettler Toledo. Periodic sampling for ion chromatography (IC) analysis further validated these measurements. To facilitate the introduction of CO_2 gas for the carbonation process, at a controlled flow rate, a gas inlet valve was integrated at the side of the reactor as shown in Figure 1. The CO_2 gas was

bubbled into the calcium-rich solution for the carbonate reaction and the supply was regulated using a mass flow controller (MFC), ensuring precise dosing. The CO_2 concentration in the solution was measured using the CO_2 sensor, CO_2NTROL Dissolved CO_2 Sensors by Hamilton Bonaduz AG (Bonaduz, Switzerland). The gas was bubbled into the solution until the partial pressure of CO_2 and thus the concentration (Section 1.3) reached 100%.

For the implementation of the autonomous process control for the selective precipitation of $CaCO_3$ from the multi-ion solution, control strategies were developed to steer the process not only towards pure $CaCO_3$ but also maximise the precipitated $CaCO_3$. The control of the precipitation process was achieved through pH regulation of the solution. The solution pH was regulated through the different dosing mechanisms of CO_2 (g) and NaOH (l). Two unique dosing mechanisms were investigated, separate dosing of CO_2 and NaOH one after the other and the other with simultaneous dosing of NaOH and CO_2, discussed in Section 0. Based on the dosing mechanisms, two distinct pH profiles have been implemented in a semi-batch experimental setup, in Figure 1, for the selective precipitation of $CaCO_3$ and to develop the control mechanisms further needed for the autonomous process chain development.

The experimental procedure involved preparing a 900 mL solution containing known concentrations of Ca^{2+} and Mg^{2+} ions, prepared by mixing $CaCl_2$ and $MgCl_2$ in different concentrations and initial concentrations measured using IC. The pH, CO_2 concentration, and Ca^{2+} ion concentration were monitored continuously using the sensors described above. The pH was first adjusted to 7, then the CO_2 was bubbled at 200 ml/min until saturation (100 % volume %) was achieved and the pH of the solution stabilized as shown in Figure 2 (a) and Figure 3 (a). Subsequently, 1M NaOH (l) was added at a rate of 9 mL/min to increase the pH and induce precipitation, with pH and Ca^{2+} concentration being monitored continuously. The NaOH addition continued with and without CO_2 addition based on the control strategy being investigated until the predefined target pH was achieved and the solution was allowed to reach a steady state. CO_2 and Ca^{2+} concentrations were continuously measured for the rate estimation, and steady-state conditions were confirmed once CO_2 concentration stabilized. Following this, alternatively or simultaneously the CO_2 and NaOH were added until next predefined saturation points until all the Ca^{2+} ion concentration in the solution was depleted to approximately 10-5 mol/L, ensuring complete precipitation of $CaCO_3$.

4.3. Characterization

The characterization of the precipitated carbonates is one of the most important steps for the selectivity analysis of $CaCO_3$ separation from a multi-ion mixture solution. The characterization was performed using a combination of analytical techniques to assess its purity, crystalline structure, thermal stability, and surface morphology. After each carbonate precipitation experiment, the solid crystals were dried and characterised by means of X-ray Diffraction (XRD), crystal size distribution, morphological and thermal analysis.

The phase purity of the precipitates was measured from the XRD spectra on a D2-Phaser diffractometer by Bruker Corporation (Massachusetts, US). equipped with a Cu anode for Kα radiation generation ($\lambda = 1.54056$ Å) at an operating voltage of 40 kV. XRD was also employed to analyse the morphology of $CaCO_3$ precipitated (i.e. Calcite, Aragonite, and Vaterite) and measure its crystal sizes. Measurements were performed in the 2θ range of 10–80° with a step size of 0.01° and scanning speed of 1s/step. The crystalline phases were identified using the Powder Diffraction File PDF-4/Minerals 2020 database from JCPDS. Previous studies [37] and [38], have also demonstrated the ability of XRD to evaluate phase transitions and the influence of reaction conditions on $CaCO_3$ polymorphs. Along with the XRD, scanning electron microscopy (SEM) imaging was used to investigate the phase morphology of the precipitated

$CaCO_3$. For this purpose, tungsten cathode-based SEM/EDX device JEOL JSM 5410 (Tokyo, Japan) was used for the imaging of the precipitated $CaCO_3$. Different magnifications were used from the range of 5000x – 10000x and at 5kV.

The particle size distribution of the precipitated $CaCO_3$ was determined using a Malvern Mastersizer 3000 laser diffraction analyser (), which employs a He-Ne laser (λ = 633 nm) and a light scattering angle of 0.02–135°. Samples were dispersed in MilliQ water to ensure well-dispersed and agglomerate-free suspensions before measurement.

Thermogravimetric analysis (TGA) was conducted to evaluate the thermal stability and decomposition behaviour of the precipitated $CaCO_3$ using a Thermal Analysis System TGA/DSC 3+ by Mettler Toledo (Ohio, USA) under a controlled nitrogen atmosphere, with a heating rate of 10°C/min from 25°C to 1000°C. The weight loss associated with CO_2 release during decomposition was used to confirm the purity of $CaCO_3$.

Along with the solid precipitate analysis, it is necessary to analyse the residual solution to close the mass balance. The concentrations of the various residual ions (Mg^{2+}, Na^{+}, Ca^{2+}, Cl^{-}) were analysed using an Ion chromatography (IC) in the post-precipitation solution. Measurements were carried out using a Thermo Scientific Dionex ICS-6000 IC system, equipped with conductivity detectors and appropriate separation columns for ion analysis. The eluents used for cation and anion separation were methane sulfonic acid (MSA) and a carbonate/bicarbonate buffer, respectively.

5. Results and Discussion

The results of the experimental procedure, using the both pH control strategies, demonstrated the implementation of the selective precipitation of pure $CaCO_3$ from different multi-ion solutions prepared from model substances and extracted mine tailings. Analysis of the precipitates and the remaining solution provided insights into the mechanisms governing the precipitation and the role of key parameters such as pH, ion concentration, impurities and CO_2 availability.

The model solutions prepared were in the concentration range of the real mine tailing exactions taken from the study by Baechle at KIT [36]. Based on this, different concentrations of Ca^{2+} ions with combination with Mg^{2+} ions as impurities were used for the $CaCO_3$ precipitation investigation as mentioned in Table 2. By bubbling CO_2 until saturation and then increasing by NaOH, the $CaCO_3$ started to precipitate at different pH conditions based on the concentration of ions in it.

Table 2: Influence of ion concentration on the precipitation pH

Ca^{2+} conc. (mol/L)	**Mg^{2+} conc. (mol/L)**	**Precipitation pH range**
0.1	0	8 – 8.5
0.1	0.05	7.5 – 8
0.1	0.1	~ 7.5
0.075	0.1	7.5 – 8
0.05	0.1	8 – 8.5

From Table 2, we can see that for higher the Ca^{2+} ion concentration, the supersaturation is achieved earlier (i.e. at lower pH) and the $CaCO_3$ precipitates soon. This is because, from

Equation 1.3 we saw that higher concentration, larger is the supersaturation factor, leading to precipitation. From the experiments, it was observed that not only the Ca^{2+} and CO_3^{2-} concentrations have an influence on the supersaturation, but also in the presence of other impurities (such as Mg^{2+}) leads to higher supersaturation, thus quicker start of the precipitation at lower pH conditions. The ion concentration analysis of the solution via IC, before and after the precipitation, revealed that the Mg^{2+} concentration did not change significantly, but the Ca^{2+} concentration reduced by a small amount. Still not all Ca^{2+} present in the solution was precipitated as $CaCO_3$. This is due to the limited availability of the CO_3^{2-} ions in the solution, dictated by the waters ability to hold dissolved CO_2 in the solution as described in Section 1. Hence to be able to precipitate all the Ca^{2+} ions in the solution as $CaCO_3$ and capture as much as CO_2 possible, more CO_2 was needed to be added to system. The goal here was that we develop an autonomous controller to carry out the precipitation process and steer the process towards maximum yield of pure $CaCO_3$. Since pH was the control variable chosen to direct the precipitation process, certain projectiles for the pH profiles as control strategies were developed. The control strategies aimed to optimize $CaCO_3$ precipitation by precisely regulating pH fluctuations and monitoring Ca^{2+} concentration in real-time.

5.1. pH Control strategies

5.1.1. pH swing strategy

The pH swing strategy is a dynamic approach used for the selective precipitation of $CaCO_3$ from the multi-ion mixture of Ca^{2+} and Mg^{2+}. This method relies on alternating acidic and basic conditions through sequential dosing of CO_2 gas and NaOH solution. A solution with 0.1M each of Ca^{2+} and Mg^{2+} was prepared for the implementation of the strategy and filled into the reactor setup shown in Figure 1. Initially, CO_2 (g) was bubbled into the solution until saturation (100% volume) was achieved, leading to a decrease in pH and further stabilization as shown in Figure 2 (a) and (b). Upon stabilization, 1 M NaOH solution was introduced at a controlled rate to elevate the pH, inducing $CaCO_3$ precipitation. The addition of NaOH continued until the pH reached 9, at which point dosing was halted, and the system was allowed to reach a steady state, in Figure 2 (a). In the Figure 2 (b) this can be seen by the increase in the Na+ concentration while the CO_2 concentration decreased. The progression of Ca^{2+} ion concentration was continuously monitored, with steady-state conditions confirmed by a minimum and stable CO_2 concentration following $CaCO_3$ formation via carbonate (CO_3^{2-}) conversion. After reaching steady-state conditions, CO_2 gas was reintroduced to re-establish acidic conditions, reducing the pH to approximately 5.8, during which while the CO_2 concentration increased, the Na+ concentration remained constant. Once saturation was achieved, NaOH was dosed again to increase the pH back to 9, repeating the cycle. This pH swing process was iterated until Ca^{2+} concentration was reduced to approximately 10-5 mol/L on the ISE, ensuring near-complete $CaCO_3$ precipitation.

Samples from both the solution and precipitates were collected at the end of steady states for further analysis. Ion concentrations were assessed using ion chromatography (IC), while the solid phase and particle size distribution (PSD) of the precipitates were characterized using the XRD and the Mastersizer, respectively.

The results confirm the effectiveness of the pH swing control strategy in achieving selective $CaCO_3$ precipitation while minimizing co-precipitation of $MgCO_3$ or $Mg(OH)_2$. This can be seen for the example of initial 0.1M each of Ca^{2+} and Mg^{2+}. In Figure 2 (a) we see by the decrease in the Ca^{2+} concentration while Mg^{2+} concentration remains almost constant throughout the precipitation process. The formation and precipitation of $CaCO_3$ can be seen

from Figure 2 (a) where we see that the Ca^{2+} concentration decreases quickly while NaOH addition due to high supersaturation and slightly increases during the CO_2 addition due to the dissolution of some of the precipitated $CaCO_3$ caused by slight undersaturation. While in Figure 2 (b), the CO_2 addition up to saturation (100% Volume %) resulting in pH decrease and for the NaOH addition, the CO_2 concentration falls to minimum due to conversion to HCO_3^- and CO_3^{2-} by acid dissociation. Also, the NaOH concentration remains constant while CO_2 addition and increases only when additional NaOH is supplied, thus showing all the Na+ ions stay in the dissolved phase and do not precipitate. The analysis of the precipitates has been discussed in the next sections.

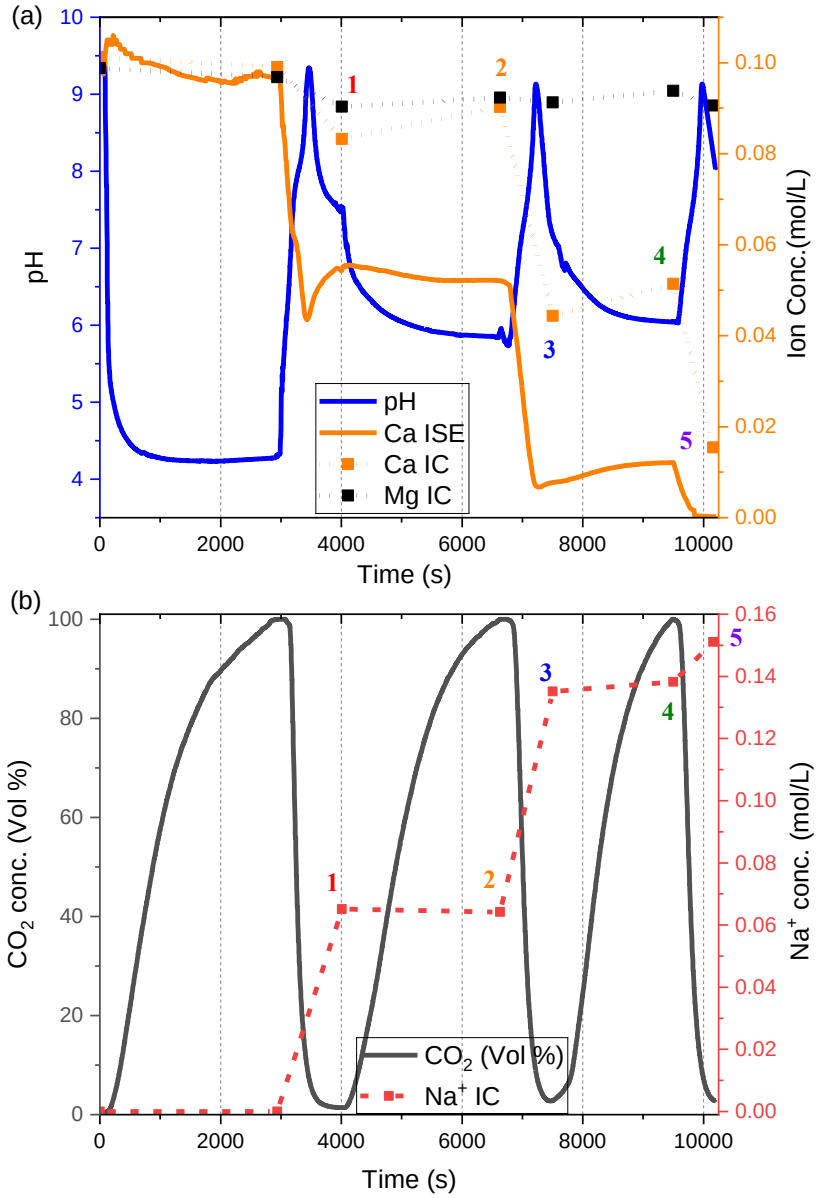

Figure 2: pH swing profile for selective precipitation of $CaCO_3$

The strategy is easy to implement and control and pure $CaCO_3$ can be precipitated. Also, the number of swings required for the near complete depletion of the Ca^{2+} ions from the solution can be predetermined based on the initial Ca^{2+} concentration and the operating pressure of the system as can be seen in Table 3. This is because of the limited amount of CO_2 the solution can hold at a particular pressure (Section 1). Table 3 also shows the decrease in the Ca^{2+} concentration at the end of each swing cycle.

Table 3: # of swings depending on the initial Ca^{2+} conc.

Initial Ca^{2+} conc. (mol/L)	# of Swings required	Ca^{2+} conc. after each swing (mol/L)					
		1	2	3	4	5	6
0.05	2	0.03666	0.00957	-	-	-	-
0.075	3	0.0565	0.02278	0.00649	-	-	-
0.1	3	0.08335	0.04433	0.01543	-	-	-
0.2	6	0.16175	0.13743	0.10542	0.08148	0.05272	0.01955
Ext. Sol. (0.063)	2	0.04523	0.01232	-	-	-	-

5.1.2. pH constant strategy

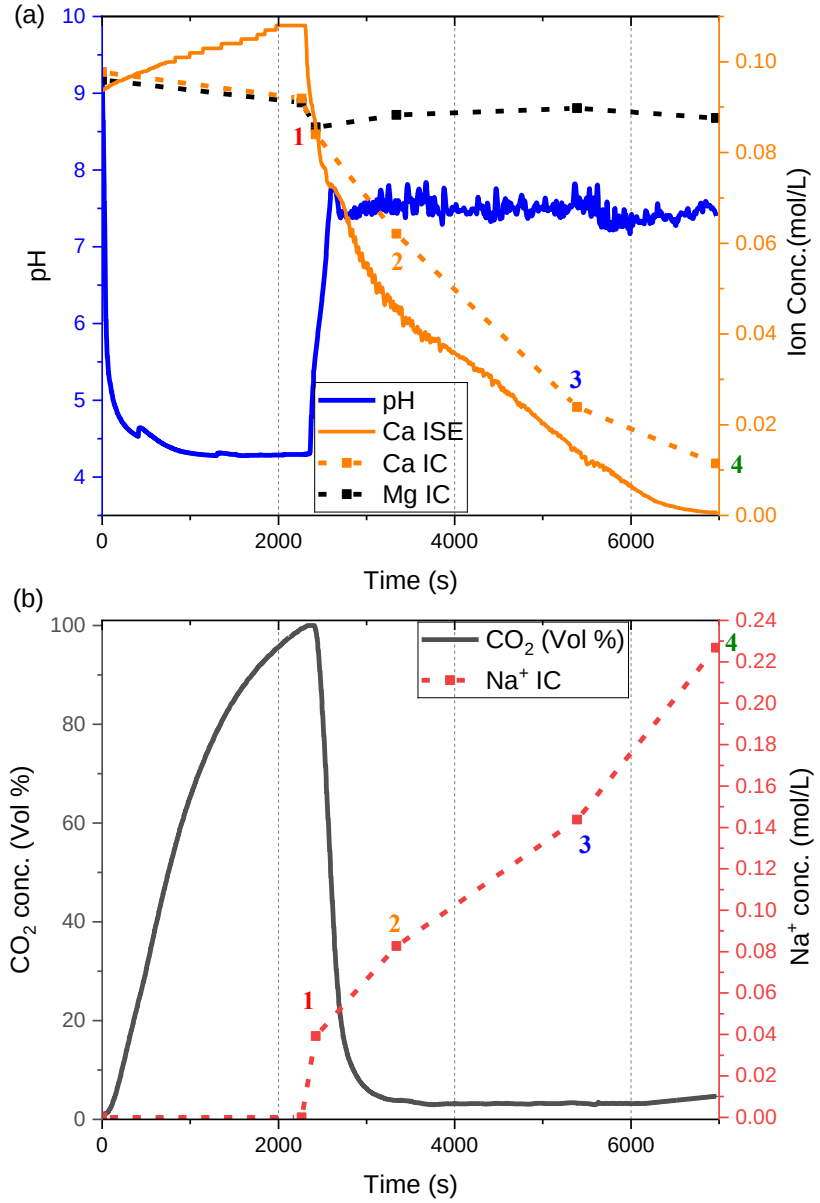

Figure 3: pH constant profile for selective precipitation of $CaCO_3$

Unlike the pH swing strategy, the pH constant strategy involves the simultaneous addition of CO_2 (g) and NaOH (l) to maintain a stable pH within the optimal range for the $CaCO_3$ precipitation Figure 3 (a) for 0.1M Ca^{2+} and 0.1M Mg^{2+} ion-rich solution. By keeping the pH constant, this approach mitigates the continuous fluctuations and provides a more controlled

environment for continuous $CaCO_3$ precipitation. As shown in Figure 3, after the first phase of CO_2 addition until saturation, the pH of the solution was raised to 7.5 by adding NaOH (l), by turning off the CO_2 (g) addition. If CO_2 (g) supply was not turned off, the pH of the solution rises very slowly initially leading to low precipitation and then the pH rises very quickly making the process uncontrollable. Hence, even for the pH constant strategy, NaOH (l) was dosed predominantly until pH 7.5. Samples are collected at this point for the analysis and precipitate characterisation. Then CO_2 (g) was bubbled continuously to the solution while maintain the pH of the solution at 7.5 by occasional dosing NaOH (l) and the precipitation was continued until the Ca^{2+} concentration fell below 10-5 mol/L on the ISE. Here since there was no back and forth shifting of the pH, the Ca^{2+} ion constantly dropped due to the precipitation of $CaCO_3$. Also, the IC measurements revealed that Mg^{2+} concentration remained constant indication no co-precipitation of magnesium compounds (see Figure 3 (a)). The analysis of the precipitated product also revealed that selective precipitation of pure $CaCO_3$. The details of the phase purity and PSD have been discussed in Section 5.2. In Figure 3 (b), while the NaOH concentration constantly increased, the CO_2 concentration remanded nearly stayed constant at pH 7.5, due to the immediate transition to the bicarbonate and carbonate ions.

5.2. pH Control strategy comparison

After the successful implementation of the both the control strategies, it was found that the strategies are suitable for precipitating $CaCO_3$ selectively. Both the strategies are equally capable of precipitating maximum amount of $CaCO_3$ from the solution while minimising the Mg^{2+} co-precipitation (see Figure 2 and Figure 3). While the pH constant method takes shorter time than the pH swing method for precipitation of $CaCO_3$, it requires larger amount of NaOH solution (about 200 ml for 0.1M Ca^{2+} initial conc.) for the precipitation leading to larger dilution of the ions present. Also, the pH constant method requires for the continuous monitoring of the Ca^{2+} ion conc. with an ISE, thus limiting the process applicability to low pressure and temperature operating conditions. While in the pH swing method depending on the initial concentration of Ca^{2+}, it can be accurately estimated the number of swings required as seen in Table 3 without the need for the constant Ca^{2+} ion monitoring. Along with these differences, the two methods also dictate the particle phase, morphology, the PSD of the precipitated $CaCO_3$ and most importantly also influences the precipitation phenomenon i.e. primary nucleation or growth of existing crystals, thus enhancing the selectivity of the precipitates formed.

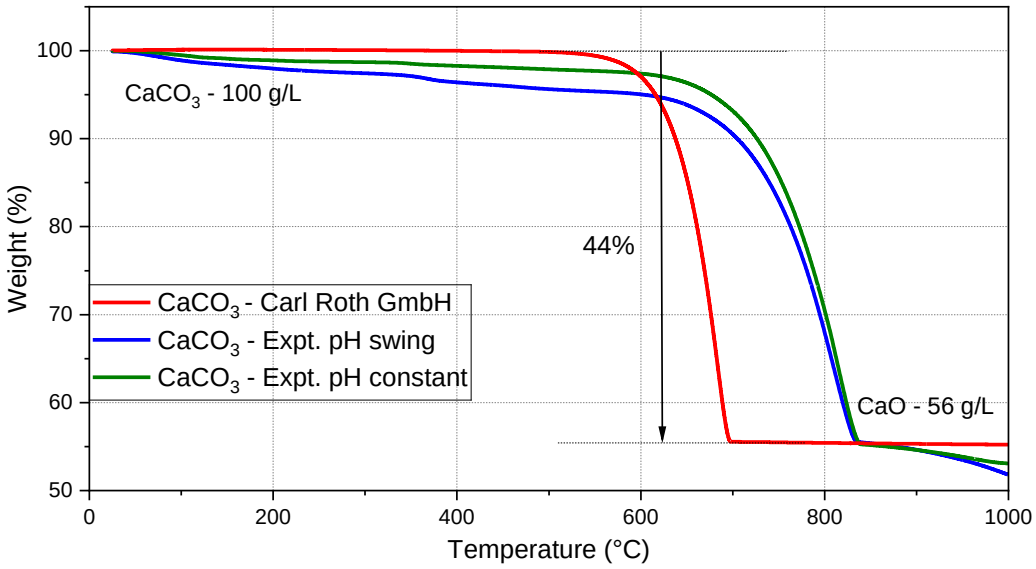

Figure 4: TGA analysis of the precipitated and ideal $CaCO_3$

To investigate the phase purity of the two precipitates formed from both the strategies, the implementation of the thermal stability analysis via TGA is shown in Figure 4, in comparison to that of the commercially available 99% pure $CaCO_3$ (from Carl Roth GmbH). The decomposition of the precipitates resulted in the approximately 44% reduction in weight which is similar to the weight loss of the ideal $CaCO_3$ (molar mass: 100 g/L) due to the decomposition on the release of CO_2 gas (molar mass: 44 g/L). As can be seen in the Figure, though the decomposition weight is in comparison to that of the commercial $CaCO_3$, the decomposition takes longer for both the precipitates formed in Mg^{2+} rich environment. This could be due to the precipitates forming large clusters making the escape of CO_2 or small amount of other substances (such as NaCl) over the surface of the precipitates. This needs further investigation and would be continued in the upcoming work.

With this analysis we identified the phase purity of the precipitates produced from both strategies, thus establishing their effectiveness. But the method offers no information about the morphology and PSD of precipitates. This has been discussed in the next sections.

5.2.1. Impact of pH control strategies on $CaCO_3$ morphology

The implementation of two distinct control strategies revealed that not only do impurities in the solution influence the phase composition of $CaCO_3$, but the reaction kinetics and pH control also play a critical role in determining particle yield. Calcium carbonate can form three different polymorphs, Calcite, Vaterite, and Aragonite, each with distinct characteristics. By applying the appropriate control strategy, the precipitation process can be steered toward the formation of specific morphologies tailored to application requirements.

Figure 5 presents the XRD measurements of precipitate samples collected at the points marked in Figure 2 and Figure 3. For the pH swing strategy, the initial precipitation at pH 9 primarily yields Calcite and Vaterite (Figure 5(a)). A similar trend is observed in the pH constant strategy, where the first NaOH addition (point 1 in Figure 3a) also results in the formation of Calcite and Vaterite (Figure 5(b)). However, as precipitation progresses, the two strategies diverge in their effects on phase composition. In the pH swing method, Calcite continues to dominate with subsequent swings, whereas in the pH constant method, Aragonite begins to emerge while Vaterite diminishes. By the end of the process, the pH swing strategy predominantly produces small Calcite particles via primary nucleation, whereas the pH constant strategy facilitates the growth of larger Aragonite particles due to secondary nucleation and growth over existing nuclei.

The morphology of these precipitated carbonates is further illustrated through SEM images in Figure 6. In Figure 6(a), Aragonite precipitated from the pH constant process exhibits a characteristic rod-like, fibrous structure, forming rosette-like aggregates [24]. In contrast, Figure 6 (b), and (c) display the Calcite and Vaterite morphologies formed via the pH swing strategy. The Calcite crystals appear as compact, densely packed rhombohedral structures, whereas Vaterite presents loosely aggregated, needle-like clusters forming star-shaped structures. These findings confirm that by carefully selecting the control strategy, both the rate of precipitation and the final morphology of $CaCO_3$ can be regulated, allowing for application-specific material synthesis.

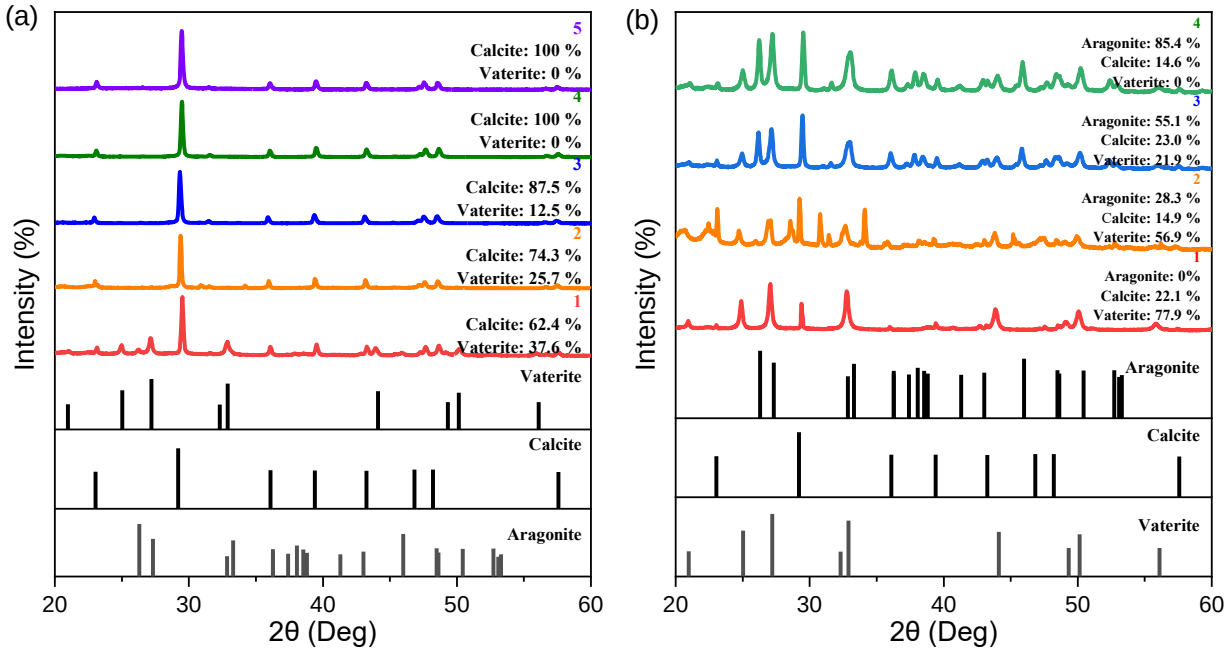

Figure 5: XRD measurements at different points (a) pH swing strategy, (b) pH constant strategy

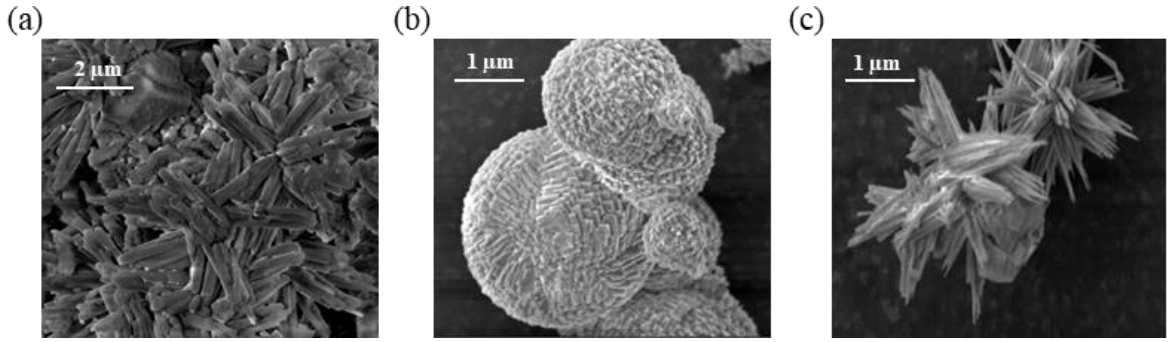

Figure 6: SEM images of the $CaCO_3$ precipitates (a) Aragonite, (b) Calcite, (c) Vaterite

5.2.2. Impact of pH control strategies on the PSD

The major impact of the control strategies is on the particle size distribution of the precipitated $CaCO_3$. We see in Figure 7 the time-dependent PSD histograms for 0.1M Ca^{2+} initial ion concentration based on the two control strategies at the different measurement points mentioned in Figure 2 and Figure *3*. In Figure 7 (a) the PSD for the pH swing strategy is shown where initially (at the measurement point 1) small particles, mean size around 1.39 µm are precipitated at pH 9 due to the addition of NaOH. Smaller particles are precipitated due to high supersaturation (Equation (4)) leading to the birth of new nucleus. On further addition of CO_2, the pH decreases resulting in undersaturation leading to the dissolution of the smallest particles. This results in the shift of the PSD causing the mean size of the particles to increase to approximately 2.4 µm, though the number of particles has reduced. On continuing the cycle of NaOH and CO_2 addition we see that very large number of small nuclei with mean size 0.9 µm are precipitated owing to the high supersaturation. Though CO_2 is added and smaller crystals dissolve, the mean size is not affected majorly due to smaller undersaturation due to the pH reduction. Also, a smaller bimodal distribution is observed that could be due to growth or aggregation of the nuclei.

On the contrary, for the pH constant strategy (in Figure 7 (b)), since the pH is held constant after the first increase, the primary nuclei formed of the similar mean size (1.42 µm), grow

(Equation (5)) over the precipitation period due to small supersaturation caused by to the continuous CO_2 addition and pH being held stable at 7.5. The process results in change of the precipitation phenomenon from primary uncontrolled nucleation to better controllable growth of the nucleated crystals. Thus, we observe a well- defined bi-modal distribution with the final mean size of over 6.6 µm.

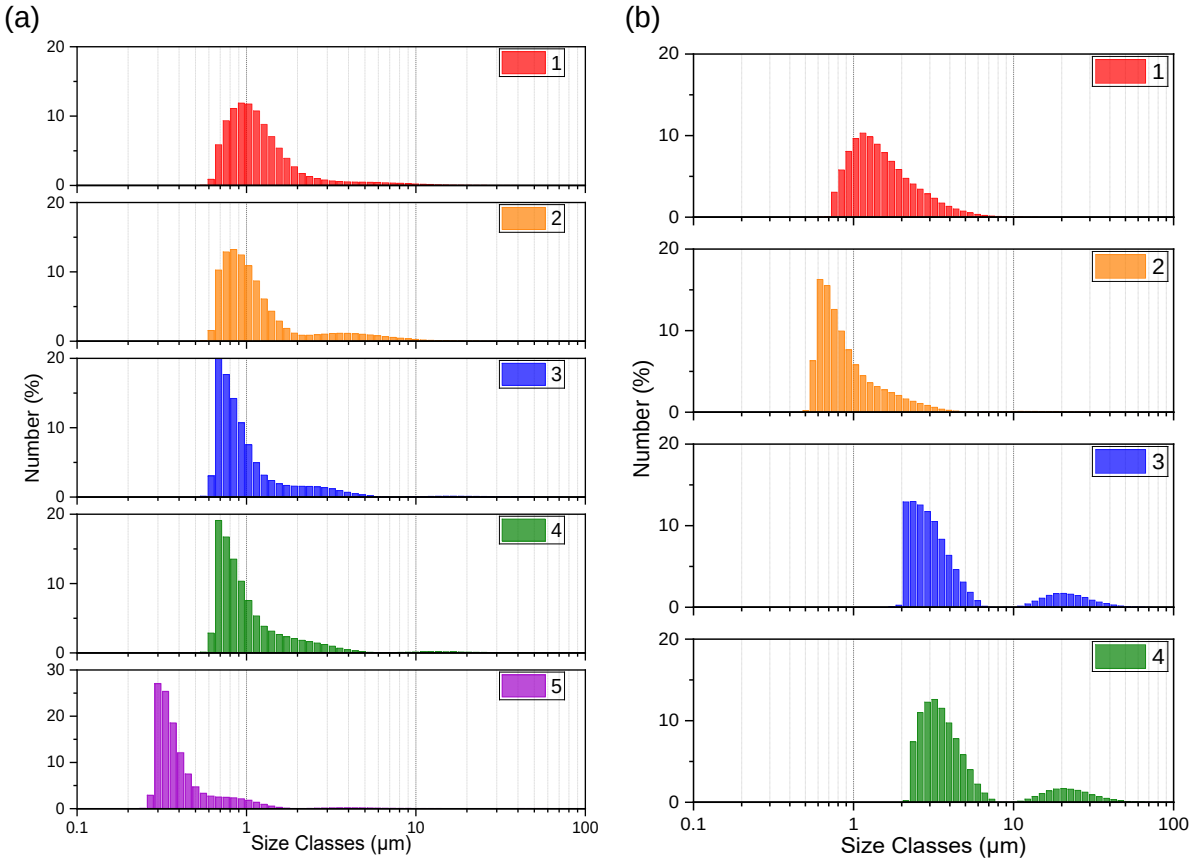

Figure 7: PSD for precipitated $CaCO_3$ through (a) pH swing, (b) pH constant strategy

In Figure 8, we see the final particle size of the precipitated $CaCO_3$ for different initial concentrations of Ca^{2+} ions at the end of the precipitation process. The Figure 8 (a) depicts the final sizes for the pH swing strategy, where we see large nucleation of very small particles due to high supersaturation. For the extraction solution also, the precipitation by the nucleation mechanism dominates. In Figure 8 (a), we also see that for higher initial concentrations of Ca^{2+} ions, the mean size shifts lower due to very large number of smaller nuclei formed spontaneously, thus indication that the supersaturation control plays a crucial role in the PSD. In Figure 8 (b) on the contrary we see that the for the pH constant strategy, the final PSD at the end of the process has shifted to larger sizes indicating a growth over the existing nuclei. The extraction solution also follows the trend indicating that this control strategy offers a better regulation of the PSD and thus the overall precipitation process.

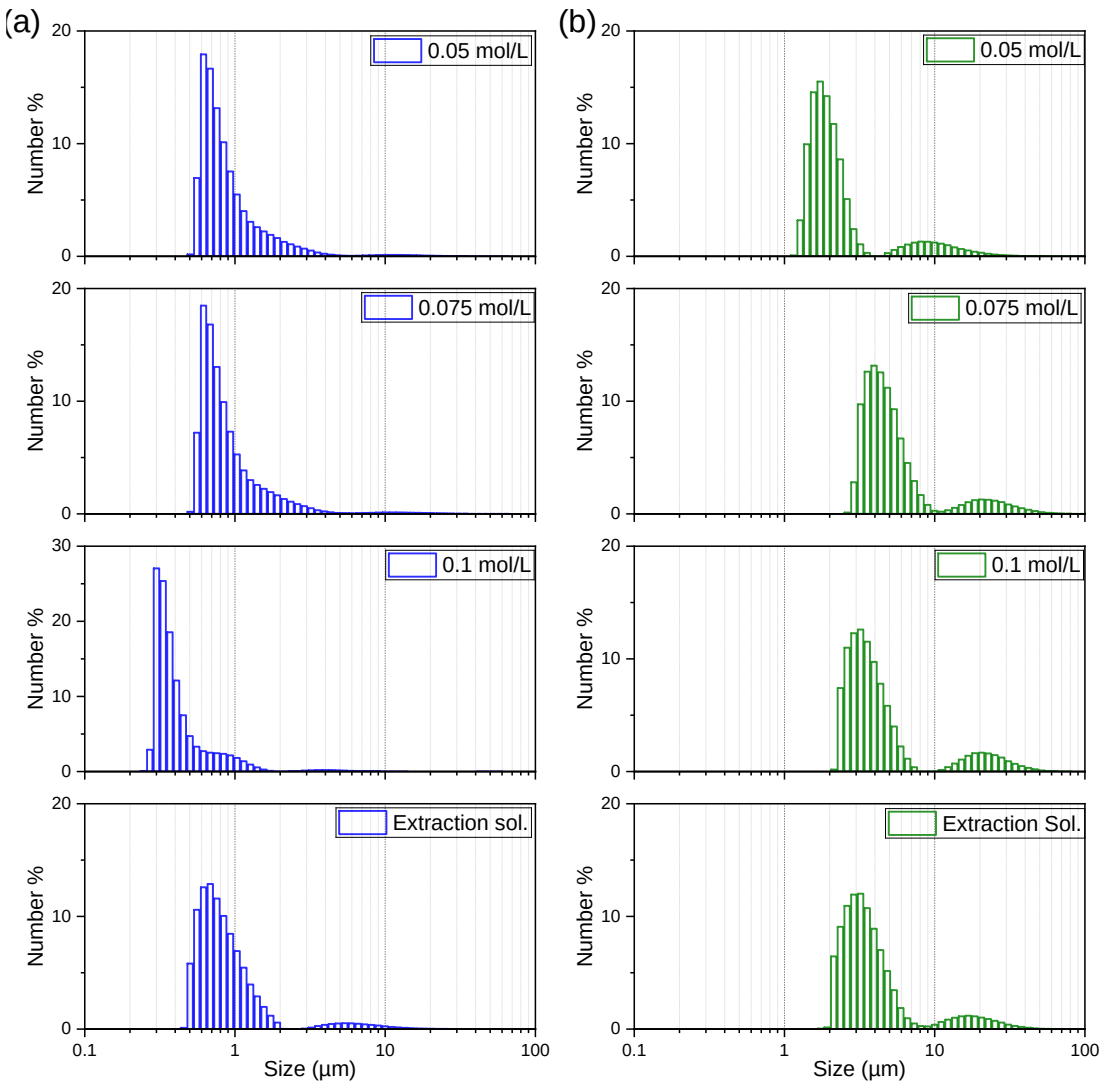

Figure 8: Comparison of different PSD for model substances and mine tailing mixture for (a) pH swing strategy, (b) pH constant strategy

6. Conclusion

In this study, we investigated the influence of pH regulation on the selective precipitation of $CaCO_3$ from a multi-ion solution. Two pH-based control strategies were developed to direct the process toward the selective formation of pure $CaCO_3$ using waste-derived solutions.

A semi-batch reactor setup with pH control was implemented to develop these strategies. Initial investigations were carried out with model solutions prepared using laboratory-grade $CaCl_2$ as the Ca^{2+} source at varying concentrations. The ability of the control strategies for the selective precipitation in the presence of impurities was examined by adding $MgCl_2$ as source of Mg^{2+} ions to the Ca^{2+}-rich solutions. The effectiveness of the control strategies was further demonstrated using actual mine tailing extraction solutions. The carbonate ions (CO_3^{2-}) was supplied through bubbling pure CO_2 gas into the solution in an open system setup at atmospheric pressure. For the pH regulation of the process, 1M NaOH was dosed. Ion concentrations were monitored over time to track the process and determine its endpoint.

Two distinct control strategies were developed: pH swing and pH constant. Based on the strategy, the morphology and particle sizes of the precipitates can be controlled. In the pH swing

strategy, the pH of the solution was lowered to 6 and increased to 9 cyclically by dosing CO_2 gas and NaOH solution respectively, until the Ca^{2+} ions in the solutions nearly depleted. Using this approach, the initially precipitated Calcite and Vaterite when subjected to cyclic precipitation and dissolution changed to completely clustered rhombohedral Calcite crystals. Rapid shift in the pH by NaOH addition to CO_2 saturated solution resulted in high supersaturation thereby causing spontaneous formation of very small particle sizes via nucleation. It was observed that for this control strategy, the number of swings (cycles) required could be predetermined based on the initial concentration of Ca^{2+} ions, without the need for continuous ion concentration monitoring, to avoid co-precipitation of other substances, thus providing simpler operational capabilities.

In contrast, the pH constant strategy, maintained a steady pH of 7.5 by continuous CO_2 dosing and intermittent NaOH addition. This method completed the process more quickly and maintained low supersaturation throughout. Due to this, the precipitation process which started initially with primary nucleation was followed by growth of the nuclei, making the process more suitable for the modelling and control purposes. Also, the Aragonite crystals dominated the morphology of the precipitated $CaCO_3$. This behaviour was consistent across different Ca^{2+} ion concentrations and with real extraction solutions, thus demonstrating the robustness and applicability of the strategy.

The model for the semi-batch process has been developed and would be presented in the future. Also, the influence of other impurities and concentrations would be investigated for development of a robust autonomous controller for the carbonation process chain.

Acknowledgement

The authors would like to thank the Deutsche Forschungsgemeinschaft (DFG, German Research Foundation) for funding the research through the SPP 2364 “Autonomous Processes in Particle Technology – Research and Testing of Concepts for Model-based Control of Particulate Processes” - project no. 504852622. Also, we would like to thank the project partners at Karlsruhe Institute of Technology (KIT) and Rhineland-Palatinate University of Technology (RPTU) for the cooperation over the autonomous control process chain development for the carbonate precipitation using mine tailings. A special thanks to Volker Baechle (KIT) for the preparation of the mine tailing extraction solutions and sending it over for the precipitation process.

7. References

[1] A. A. Khosa, T. Xu, B. Q. Xia, J. Yan, and C. Y. Zhao, “Technological challenges and industrial applications of CaCO3/CaO based thermal energy storage system – A review,” Solar Energy, vol. 193, pp. 618–636, Nov. 2019, doi: 10.1016/j.solener.2019.10.003.

[2] “Calcium carbonate - what is this substance and what is it mainly used for? | Foodcom S.A.” Accessed: Mar. 23, 2025. [Online]. Available: https://foodcom.pl/en/calcium-carbonate-what-is-this-substance-and-what-is-it-mainly-used-for/

[3] “What is calcium carbonate and what is it used for? - PCC Group Product Portal.” Accessed: Mar. 23, 2025. [Online]. Available: https://www.products.pcc.eu/en/blog/what-is-calcium-carbonate-and-what-is-it-used-for/

[4] "Major Industrial Applications use CaCO3 calcium carbonate in everyday life." Accessed: Mar. 23, 2025. [Online]. Available: https://www.linkedin.com/pulse/major-industrial-applications-use-caco3-calcium-carbonate-
[5] "The Role of Calcium Carbonate Powder in Industrial Applications." Accessed: Mar. 23, 2025. [Online]. Available: https://sudarshangroup.com/the-role-of-calcium-carbonate-powder-in-industrial-applications/
[6] "Calcium Carbonate Uses in Industry: Things You Need to Know." Accessed: Mar. 23, 2025. [Online]. Available: https://elchemy.com/blogs/food-nutrition/top-industrial-uses-of-calcium-carbonate-applications-across-multiple-sectors
[7] "Calcium Carbonate | Plastic Resins |." Accessed: Mar. 23, 2025. [Online]. Available: https://www.plasticservice.com/industry-news/7062/industrial-uses-of-calcium-carbonate
[8] K. V. Gomes, C. M. Woodall, H. Pilorgé, P. Psarras, and J. Wilcox, "Techno-economic analysis of indirect carbonation processes for carbon sequestration using mining waste," Energy Advances, 2025, doi: 10.1039/d4ya00567h.
[9] A. Azdarpour, M. Asadullah, E. Mohammadian, H. Hamidi, R. Junin, and M. A. Karaei, "A review on carbon dioxide mineral carbonation through pH-swing process," Nov. 01, 2015, Elsevier. doi: 10.1016/j.cej.2015.05.064.
[10] A. A. Olajire, "A review of mineral carbonation technology in sequestration of CO2," J Pet Sci Eng, vol. 109, pp. 364–392, Sep. 2013, doi: 10.1016/j.petrol.2013.03.013.
[11] E. R. Bobicki, Q. Liu, Z. Xu, and H. Zeng, "Carbon capture and storage using alkaline industrial wastes," Prog Energy Combust Sci, vol. 38, no. 2, pp. 302–320, Apr. 2012, doi: 10.1016/j.pecs.2011.11.002.
[12] Y. P. Lin and P. C. Singer, "Inhibition of calcite precipitation by orthophosphate: Speciation and thermodynamic considerations," Geochim Cosmochim Acta, vol. 70, no. 10, pp. 2530–2539, May 2006, doi: 10.1016/J.GCA.2006.03.002.
[13] M. F. Hochella et al., "Nanominerals, mineral nanoparticles, and earth systems," Science (1979), vol. 319, no. 5870, pp. 1631–1635, Mar. 2008, doi: 10.1126/SCIENCE.1141134.
[14] G. Falini, S. Fermani, G. Tosi, and E. Dinelli, "Calcium carbonate morphology and structure in the presence of seawater ions and humic acids," Cryst Growth Des, vol. 9, no. 5, pp. 2065–2072, May 2009, doi: 10.1021/cg8002959.
[15] D. Kralj, J. Kontrec, L. Brečević, G. Falini, and V. Nöthig-Laslo, "Effect of Inorganic Anions on the Morphology and Structure of Magnesium Calcite," Chemistry - A European Journal, vol. 10, no. 7, pp. 1647–1656, Apr. 2004, doi: 10.1002/chem.200305313.
[16] E. J. Zeller and J. L. Wray, "Factors Influencing Precipitation of Calcium Carbonate," Am Assoc Pet Geol Bull, vol. 40, no. 1, pp. 140–152, Jan. 1956, doi: 10.1306/5CEAE30A-16BB-11D7-8645000102C1865D.
[17] A. H. A. Park, R. Jadhav, and L. S. Fan, "CO2 Mineral Sequestration: Chemically Enhanced Aqueous Carbonation of Serpentine," Can J Chem Eng, vol. 81, no. 3–4, pp. 885–890, Jun. 2003, doi: 10.1002/CJCE.5450810373.
[18] "The Effect of pH on Nucleation Kinetics in Solutions".
[19] N. Saksono, S. Bismo, R. W. Soemantojo, and A. Manaf, "Effects of pH on Calcium Carbonate Precipitation under Magnetic field," 2009.
[20] A. Millan, F. Grases, O. Söhnel, and I. Křivánková, "Semi-Batch Precipitation of Calcium Oxalate Monohydrate," Crystal Research and Technology, vol. 27, no. 1, pp. 31–39, Jan. 1992, doi: 10.1002/CRAT.2170270105.

[21] C. Steyer, M. Mangold, and K. Sundmacher, “Modeling of particle size distribution for semibatch precipitation of barium sulfate using different activity coefficient models,” Ind Eng Chem Res, vol. 49, no. 5, pp. 2456–2468, Mar. 2010, doi: 10.1021/IE901306R.
[22] B. Han, H. Qu, H. Niemi, Z. Sha, and M. Louhi-Kultanen, “Mechanistic study of magnesium carbonate semibatch reactive crystallization with magnesium hydroxide and CO2,” Ind Eng Chem Res, vol. 53, no. 30, pp. 12077–12082, Jul. 2014, doi: 10.1021/ie501706j.
[23] Z. Hu et al., “Synthesis of Needle-Like Aragonite Crystals in the Presence of Magnesium Chloride and Their Application in Papermaking,” Advanced Composite Materials, vol. 18, no. 4, pp. 315–326, Oct. 2009, doi: 10.1163/156855109X434720.
[24] G. Falini, S. Fermani, G. Tosi, and E. Dinelli, “Calcium carbonate morphology and structure in the presence of seawater ions and humic acids,” Cryst Growth Des, vol. 9, no. 5, pp. 2065–2072, May 2009, doi: 10.1021/cg8002959.
[25] L. Filipescu, “Semi-batch Reactive Precipitation of Calcium Carbonate.” Accessed: Mar. 24, 2025. [Online]. Available: https://www.academia.edu/20107593/Semi_Batch_Reactive_Precipitation_Of_Calcium_Carbonate
[26] F. Liendo, M. Arduino, F. A. Deorsola, and S. Bensaid, “Nucleation and growth kinetics of CaCO3 crystals in the presence of foreign monovalent ions,” J Cryst Growth, vol. 578, Jan. 2022, doi: 10.1016/j.jcrysgro.2021.126406.
[27] O. Söhnel and J. W. Mullin, “Precipitation of calcium carbonate,” J Cryst Growth, vol. 60, no. 2, pp. 239–250, Dec. 1982, doi: 10.1016/0022-0248(82)90095-1.
[28] H. Qian, X. Zhang, and P. Li, “Calculation of CaCO3 Solubility (Precipitability) in Natural Waters,” Asian Journal of Chemistry, vol. 24, pp. 668–672, Feb. 2012.
[29] T. E. Larson, F. W. Sollo, F. F. Mcgurk, and T. E. Larson, “Complexes Affecting The Solubility Of Calcium Carbonate In Water Wrc Research Report No. 68 Complexes Affecting The Solubility Of Calcium Carbonate In Water,” 1973.
[30] W. Zhao, B. Han, K. Jakobsson, M. Louhi-Kultanen, and V. Alopaeus, “Mathematical model of precipitation of magnesium carbonate with carbon dioxide from the magnesium hydroxide slurry,” Comput Chem Eng, vol. 87, pp. 180–189, Apr. 2016, doi: 10.1016/j.compchemeng.2016.01.013.
[31] J. Hostomsky and A. G. Jones, “A penetration model of the gas-liquid reactive precipitation of calcium carbonate crystals,” Chemical Engineering Research and Design, vol. 73, no. A3, pp. 241 – 245, 1995, [Online]. Available: https://www.scopus.com/inward/record.uri?eid=2-s2.0-0029288221&partnerID=40&md5=008318b8dea090e831a57b9638ab4fd6
[32] J. J. Middelburg, “Biogeochemical Processes and Inorganic Carbon Dynamics,” pp. 77–105, 2019, doi: 10.1007/978-3-030-10822-9_5.
[33] “Carbon dioxide.” Accessed: Mar. 24, 2025. [Online]. Available: https://webbook.nist.gov/cgi/cbook.cgi?ID=C124389&Mask=10
[34] D. Pabsch, C. Held, and G. Sadowski, “Modeling the CO2Solubility in Aqueous Electrolyte Solutions Using ePC-SAFT,” J Chem Eng Data, vol. 65, no. 12, pp. 5768–5777, Dec. 2020, doi: 10.1021/acs.jced.0c00704.
[35] “39.5: Gas Exchange across Respiratory Surfaces - Gas Pressure and Respiration - Biology LibreTexts.” Accessed: Mar. 24, 2025. [Online]. Available: https://bio.libretexts.org/Bookshelves/Introductory_and_General_Biology/General_Biology_(Boundless)/39%3A_The_Respiratory_System/39.05%3A_Gas_Exchange_across_Respiratory_Surfaces_-_Gas_Pressure_and_Respiration

[36] V. Bächle, C. Hegde, A. Voigt, K. Sundmacher, and M. Gleiß, “Tailings as a Source for Generating valuable Magnesium and Calcium Carbonates by Leaching and Carbonization,” Mar. 14, 2025. doi: 10.26434/chemrxiv-2025-cjxfm.

[37] R. Ševčík, P. Šašek, and A. Viani, “Physical and nanomechanical properties of the synthetic anhydrous crystalline CaCO3 polymorphs: vaterite, aragonite and calcite,” J Mater Sci, vol. 53, no. 6, pp. 4022–4033, Mar. 2018, doi: 10.1007/s10853-017-1884-x.

[38] K. Song, J. H. Bang, S. C. Chae, J. Kim, and S. W. Lee, “Phase and morphology of calcium carbonate precipitated by rapid mixing in the absence of additives,” RSC Adv, vol. 12, no. 30, pp. 19340–19349, Jul. 2022, doi: 10.1039/d2ra03507c.

[39] P. Gao and Y. Shi, “Characterization of supersaturatable formulations for improved absorption of poorly soluble Drugs,” Dec. 2012. doi: 10.1208/s12248-012-9389-7.

[40] J. D. Naviaux, A. V. Subhas, N. E. Rollins, S. Dong, W. M. Berelson, and J. F. Adkins, “Temperature dependence of calcite dissolution kinetics in seawater,” Geochim Cosmochim Acta, vol. 246, pp. 363–384, Feb. 2019, doi: 10.1016/j.gca.2018.11.037.

[41] G. Guner, A. Amjad, M. Berrios, M. Kannan, and E. Bilgili, “Nanoseeded Desupersaturation and Dissolution Tests for Elucidating Supersaturation Maintenance in Amorphous Solid Dispersions,” Pharmaceutics, vol. 15, no. 2, Feb. 2023, doi: 10.3390/pharmaceutics15020450.